VDMA
Fluid Power Association

23rd ISC

International Sealing Conference

Stuttgart, Germany
Sept.30 - Oct.1, 2026

Sealing the future –
Facing the challenges of tomorrow

UNI STUTTGART

Fachverband Fluidtechnik im VDMA e. V. Lyoner Str. 18
50628 Frankfurt am Main
Germany

Phone +49 69 6603-1513
E-Mail maximilian.baxmann@vdma.eu

Internet www.vdma.eu/fluid

Interactions between elastomeric materials and lithium-ion batteries

Sandra Kofink, Marc Gay

The long-term reliability of lithium-ion battery (LIB) assemblies depends not only on electrolyte formulation and electrode design but also on the chemical compatibility of sealing materials that remain in continuous contact with the electrolyte. Although elastomers are essential components in pouch cells, cylindrical headers and module interfaces, the interactions between them and the electrolyte have received comparatively little attention. As lithium hexafluorophosphate ($LiPF_6$)-based electrolytes are known to be chemically sensitive to impurities, moisture and catalytic surfaces, interactions with elastomeric components may promote degradation pathways that ultimately affect cell performance. This study evaluates four elastomers, two fluorocarbon rubbers (FKM) and two ethylene propylene diene monomers (EPDM), by aging them in $LiPF_6$-based electrolyte and assessing their chemical compatibility as well as their impact on the electrolyte and the electrochemical performance of cells. The aged electrolyte was analyzed via Inductively Coupled Plasma Optical Emission Spectroscopy (ICP-OES), Ion Chromatography (IC), High-Performance Liquid Chromatography-Mass Spectrometry (HPLC-MS) and colorimetry to determine the potential release of inorganic and organic impurities from the elastomer, along with information about the degree of decomposition of the electrolyte itself. Clear differences in material compatibility were observed. Only one of the tested compounds showed minimal reactivity: impurity levels remained low, difluorophosphate formation was limited and no additional organic decomposition species were detected. To connect chemical compatibility with functional cell behavior, electrolytes aged with each elastomer were subsequently evaluated in electrochemical tests. Electrochemical performance was assessed by measuring internal resistance, voltage hysteresis, voltaic efficiency and capacity retention during cycling, highlighting the importance of choosing an appropriate sealing material.

1 Introduction

Lithium-ion batteries (LIB) are used in many modern energy storage applications, ranging from portable electronics to, most prominently, electric mobility. High energy density, long cycle life and a relatively low self-discharge rate are the main aspects that led to widespread commercialization. The electric vehicle market in particular has been a key driver of the lithium-ion battery demand. [1]

Electric vehicles currently account for 70-85% of total lithium-ion battery use, making them the main end-use segment. One in four newly sold vehicles globally was electric in 2025, and the market is still growing at a compound annual growth rate (CAGR) of 22.2% from 2025 to 2030.[2], [3], [4]

Automotive applications require service lifetimes of 10-15 years. Degradation processes such as electrolyte decomposition can lead to capacity fade, increased internal resistance and overall reduced efficiency. Factors such as temperature, cycling

conditions, contamination and interactions between different components within the cell can influence this. [5]

Electrolytes are typically based on lithium hexafluorophosphate ($LiPF_6$) dissolved in mixtures of organic carbonates. Despite their electrochemical stability, their thermal and chemical stability suffers under certain conditions, particularly in contact with moisture or reactive surfaces. When decomposition occurs, hydrofluoric acid (HF) and fluorophosphate species form. [6]

While there is a strong focus on the choice and development of electrode materials and electrolyte formulations, other components such as sealing materials receive little attention.

Whether cylindrical, prismatic or pouch cells, seals are an essential part of the battery design. They ensure electrolyte containment and prevent moisture ingress.

Elastomeric sealing materials currently used in battery cells include fluorocarbon rubbers (FKMs) and ethylene propylene diene monomers (EPDMs). The base material classes already differ greatly in their properties, and even within a material class the interactions between electrolyte and elastomer can be adjusted through different recipes.

2 Properties relevant for battery sealing

Elastomers used as sealing materials must satisfy a range of requirements, which can be grouped into five categories: electrical, thermal, media-related, permeation-related and other functional requirements, as summarized in Table 1. These specifications derive primarily from both customer expectations and broader market demands, which define the operating conditions and performance criteria for the sealing system.

Table 1: Overview of typical requirements for elastomeric materials for battery cells.

Requirement	Description
Electrical	Sufficient surface and volume resistivity
Thermal	Resistant in typical application temperature range of LIB (-40 °C to +85 °C)
Media	Resistant against the electrolyte
Permeation	Prevent moisture penetration and gases from escaping
Other	Compatibility with copper and aluminum, low leach-out, no influence on cell performance

Regarding electrical properties, volume resistivity serves as an initial indicator of whether a material is suitable for use as an insulator. Additional relevant parameters include dielectric strength and the comparative tracking index. Thermal requirements define the temperature range within which the material must remain stable and retain its functional properties.

Furthermore, the material must exhibit sufficient resistance against electrolytes in both the liquid and gaseous state. Since neither moisture should penetrate the cell nor gases escape from it, the material must demonstrate a low permeation rate.

In addition, polymeric materials may interact with metallic components. Because the sealing elements are in contact with the current collector, their chemical compatibility with metals must be ensured to prevent degradation or adverse reactions.

This paper subsequently investigates the interactions between selected elastomers and the electrolyte, with particular emphasis on their effects on battery cell performance.

3 Materials

Based on previous research, different types of FKM are predominantly found in battery cells today. Regarding chemical compatibility with the solvent used in electrolytes, EPDM was expected to perform better. Therefore, two FKMs and two EPDMs were tested in this study.

Table 2: Overview of the materials used in this study.

Material class	Reference	Hardness	Temperature range	Base filler
EPDM	EPDM 1	60 Shore A	-45 °C to +150 °C	Silica
	EPDM 2	70 Shore A	-45 °C to +150 °C	Carbon black
FKM	FKM 1	60 Shore A	-20 °C to +200 °C	Barium
	FKM 2	70 Shore A	-5 °C to +200 °C	Silica

The elastomers differed in the base material as well as the main filler used. In general, all four have a low plasticizer content to reduce the potential leach-out of substances that could influence battery performance.

The electrolyte used in this study consisted of 1.0 M $LiPF_6$ dissolved in ethylene carbonate:ethylene methylene carbonate (EC:EMC) (3:7, by weight) with 2 wt.% vinylene carbonate (VC), referred to as LP572 in the following chapters.

4 Methods

The following sections describe the methods used to analyze material compatibility, the electrolyte and battery performance.

4.1 Analysis of material compatibility

To determine the chemical compatibility of the four materials, we performed an immersion test in the electrolyte.

First, we measured the hardness, volume, weight, tensile strength and elongation at break. The samples were dried for 16 h at +40 °C in a vacuum oven to remove any remaining moisture, which is known to degrade the electrolyte. They were placed in vessels filled with electrolyte, which were then closed and stored at the respective temperature for a specific period. Afterward, the samples were removed from the vessel, cleaned with EC:EMC solution and measured for weight and volume. The samples were dried in a vacuum oven for 48 h at +40 °C before weight and volume were measured again. In addition, the hardness, tensile strength and elongation at break were tested so that change values could be calculated.

Some of the samples were analyzed via Scanning Electron Microscope with Energy Dispersive Spectroscopy (SEM-EDS) to determine the composition and presence of substances found on the surface as well as inside some samples.

For this paper, only the results of immersion for 1,512 h at +25 °C and +80 °C were considered. Further immersion tests at different temperatures were conducted but are not part of this study.

4.2 Analysis of the electrolyte

The electrolyte was analyzed via several methods. The free acid content, which indicates degradation of the electrolyte, was determined via acid-base titration.

In addition to a visual analysis of the change in color of the electrolyte, color determination was performed according to ASTM D1209 to quantify the changes.

To determine the kind and quantity of anions and cations washed out of the elastomer, Inductively Coupled Plasma Optical Emission Spectroscopy (ICP-OES) and Ion Chromatography (IC) were performed, limited to the expected ions from the compounds as well as the ions suspected of influencing battery performance. [7]

To determine the organic contaminations in the electrolyte after the elastomers were immersed, High-Performance Liquid Chromatography-Mass Spectrometry (HPLC-MS) was performed.

4.3 Measurement of battery performance

To evaluate the effect of the electrolyte, which had been in contact with the elastomer samples at +80 °C for 1,512 h, on the performance of a battery cell, this aged electrolyte was used to fill pouch cells (capacity 240 mAh, graphite negative electrode/NMC811 positive electrode). In addition, cells were filled with the aged reference electrolyte from the immersion tests, which had not come into contact with any elastomer, and with a fresh, unused electrolyte.

These cells were subsequently cycled for 300 cycles at +25 °C. Cycling refers to the repeated charging and discharging of the cells under defined operating conditions. This affects the internal resistance due to the continuous degradation of electrode and/or electrolyte components. Therefore, Hybrid Pulse Power Characterization (HPPC) tests are conducted every 45 cycles at different states of charge (SOC) to

monitor resistance development. Performance was evaluated by comparing the relative discharge capacity and internal resistance of the individual cells.

5 Results

The following sections discuss the interactions between elastomeric materials and electrolyte and their effects on the material itself, on the electrolyte and on battery performance.

5.1 Effect on the material

The samples after immersion at +80 °C, before and after redrying, are shown in Figure 1. Considerable degradation was visible on the surface of EPDM 1. The color turned dark, and after redrying some crystalline substance was found on the surface. In general, both EPDMs had a small change in volume during immersion as well as after redrying. The FKMs, on the other hand, showed extreme swelling during immersion (Figure 2 and Figure 3).

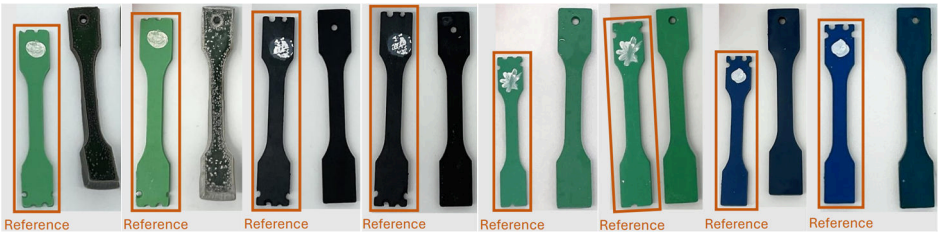

Figure 1: Visual representation of the volume change of samples right after immersion for 1,512 h at +80 °C and after redrying in a vacuum oven. Left to right: EPDM 1, EPDM 2, FKM 1, FKM 2.

After redrying some volume change was still visible, especially at +80 °C. The initial volume change of FKM 1 increased by only 20% from +25 °C to +80 °C, whereas the volume change of FKM 2 doubled. In addition, FKM 2 and EPDM 1 had a significantly higher weight change at +80 °C compared to +25 °C.

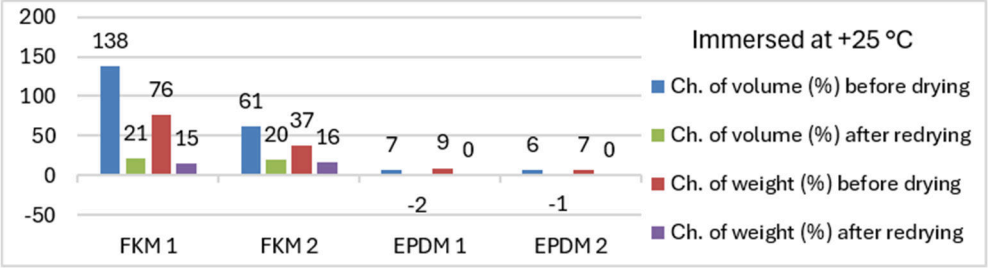

Figure 2: Change in volume and weight right after immersion at +25 °C as well as after redrying for 48 h at +40 °C in a vacuum oven.

After immersion for 1,512 h at +25 °C, there was no significant change of properties for the two EPDMs. The FKMs, on the other hand, showed a significant decrease in hardness and tensile strength. This can be explained by the remaining volume change after the first drying process. The FKMs were therefore dried a second time and their mechanical properties measured once again. The second drying led to a decrease in change values, which indicates that this was less of a permanent chemical attack and more a reversible physical change.

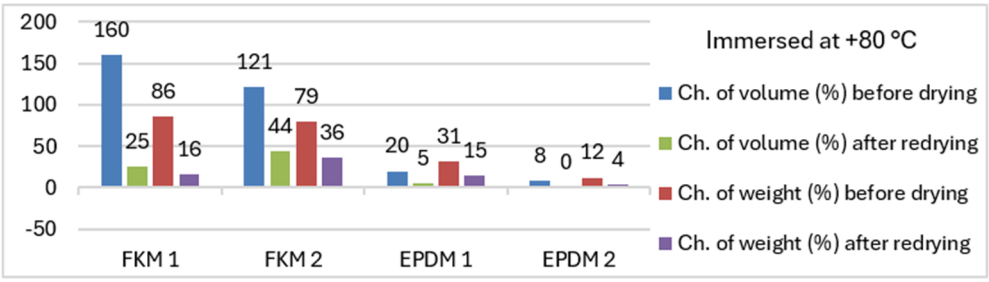

Figure 3: Change in volume and weight right after immersion at +80 °C as well as after redrying for 48 h at +40 °C in a vacuum oven.

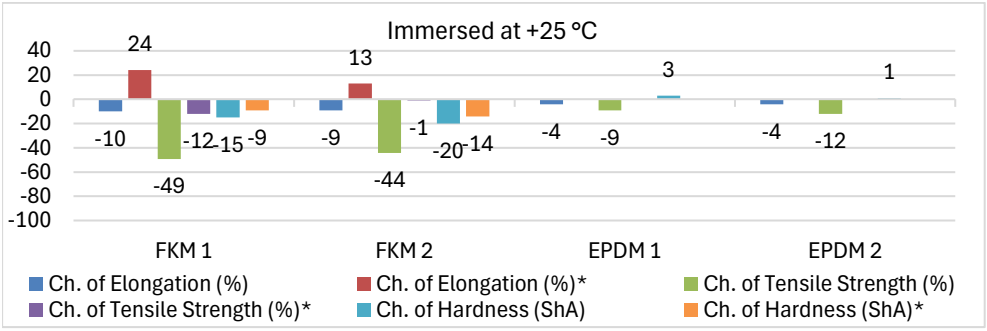

Figure 4: Change in properties after immersion for 1,512 h at +25 °C and redrying for 48 h at +40 °C in a vacuum oven, plus an additional 16 h at +100 °C for the FKMs.*

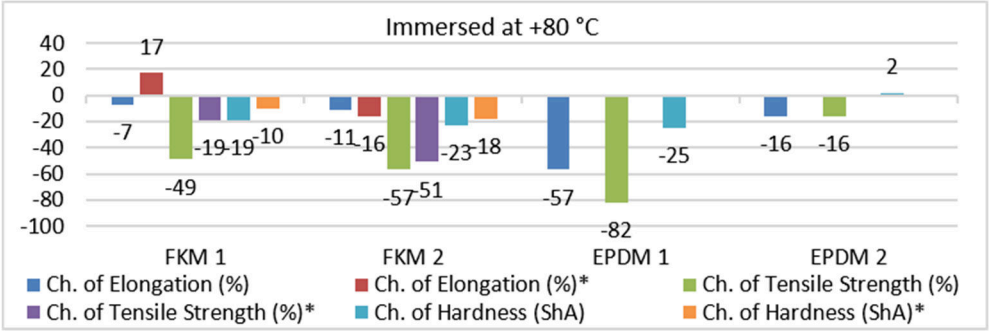

Figure 5: Change in properties after immersion for 1,512 h at +80 °C and redrying for 48 h at +40 °C in a vacuum oven, plus additional 16 h at +100 °C for the FKMs.*

At +80 °C the results differ. EPDM 1 had a reduction in mechanical properties of 57% for elongation at break and 82% for tensile strength, which clearly shows degradation (Figure 5). The reduced properties of FKM 2 did not improve through the second redrying process as they did at +25 °C which indicates that this material also experienced degradation.

Analysis of EPDM 1 via SEM-EDS was performed to further understand the reaction at +80 °C. A crust formed on the surface, consisting of fluorine and silica. Phosphorus was found inside of the compound (Figure 6).

Potential reactions that could have occurred are shown below:

$$LiPF_6 \rightleftharpoons LiF + PF_5$$
$$PF_5 + H_2O \rightarrow POF_3 + 2HF$$
$$SiO_2 + 4HF \rightarrow SiF_4 + 2H_2O$$

In $LiPF_6$-based EC:EMC electrolytes, elevated temperatures promote salt decomposition to PF_5 and LiF. In the presence of trace moisture, PF_5 forms HF and POF_3. HF can then attack the silica filler (SiO_2), generating fluorosilicone species such as SiF_4 or hexafluorosilicate-type species, while simultaneously self-accelerating electrolyte degradation.

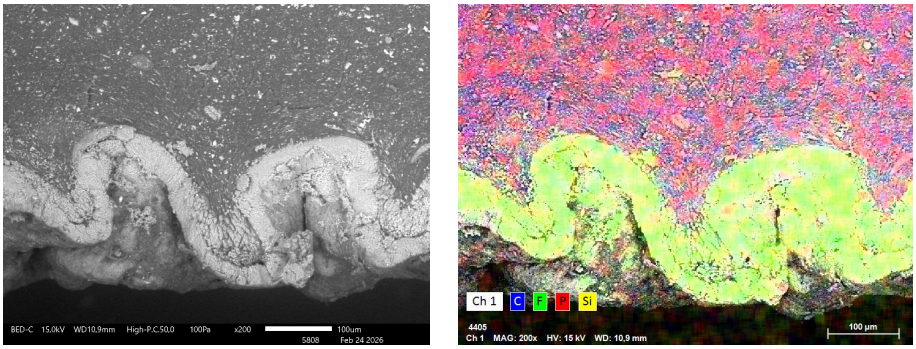

Figure 6: SEM-EDS image of a cross section of EPDM 1 immersed for 1,512 h at +80 °C.

As the two FKMs showed different behavior in respect to swelling and chemical resistance, their cross sections were also analyzed (Figure 7). FKM 1 showed traces of phosphorus inside, but the barium-based filler was the main component detected.

FKM 2, on the other hand, changed significantly. Large clusters based on phosphorus and oxygen were visible, as were holes in place of the silica filler that was clearly embedded in the polymer matrix in the initial cross section.

The fact that the silica in EPDM 1 mostly reacted on the surface, whereas the silica throughout the whole FKM 2 compound reacted, could be explained by the swelling behavior. The swelling of FKM leads to a widened network, which enables internal formation and accumulation of phosphorus-containing decomposition products and internal consumption of the silica filler, rather than the formation of a single outer Si/F crust.

With the filler consumed in the reaction, the noticeable decrease in mechanical properties is explained.

Even though FKM 1 expands more, only insignificant amounts of phosphorus were found in the network after redrying. This could be because the filler is less soluble or because it is less reactive and therefore remains in the network without giving phosphate salts the space to form and accumulate.

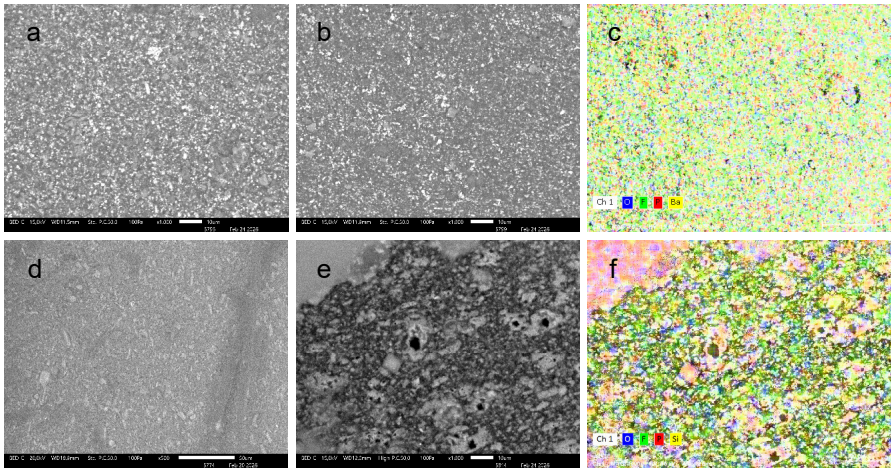

Figure 7: SEM image and EDS mapping of cross sections of FKM 1 before immersion (a) and after immersion at +80 °C (b, c), and of FKM 2 before immersion (d) and after (e, f).

5.2 Effect on the electrolyte

The color of the electrolyte is often used as a quality criterion. In the immersion tests, the color of the electrolyte changed significantly during exposure to +80 °C, even without contact with the elastomers. Figure 8 and the color determination results (Table 3) show that the least change occurred in the liquid with EPDM 2, followed by the stored reference and FKM 1. The electrolyte in contact with EPDM 1 and FKM 2 appeared almost black.

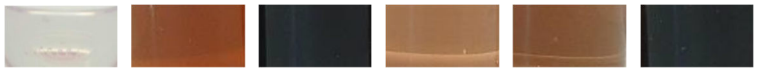

Figure 8: Electrolyte after 1,512 h at +80 °C in contact with the four elastomers. Left to right: fresh reference, stored reference, EPDM 1, EPDM 2, FKM 1, FKM 2.

Another parameter often used to determine the quality and degradation of an electrolyte is the free acid content. The measurements align with the findings above in the SEM-EDS analysis and with the basic underlying reaction of self-accelerating decomposition. The difference between +25 °C and +80 °C immersion indicates that the reaction is temperature dependent.

The element analysis performed by ICP-OES showed that most investigated elements were detected at concentrations below 1 mg/kg and are therefore marked as

"-" in Table 4, except for the electrolyte in which EPDM 1 and FKM 2 were immersed. The electrolyte of EPDM 1 showed 4 mg/kg silica, and the electrolyte of FKM 2 6 mg/kg silica in addition to 5 mg/kg calcium, which can be explained in both cases by the reaction of the filler

Table 3: Results of color determination and analysis of free acid content for fresh and stored electrolyte as well as electrolyte in contact with the different samples.

Analysis	T	Fresh reference	Stored reference	EPDM 1	EPDM 2	FKM 1	FKM 2
Pt-Co color unit	+80 °C	9	694	18,560	463	1,694	10,278
Free acid content (ppm)	+25 °C	-	59	233	70	248	95
	+80 °C	-	633	2,760	368	897	1,949

Furthermore, the IC measurement revealed an increase in DFP^- in the electrolyte in contact with EPDM 1 and FKM 2, whereas the results of EPDM 2 and FKM 1 were similar to the stored reference. DFP^- is created in the electrolyte degradation process, but is also known to enhance battery performance, which must be considered in the next section.

Table 4: Results of ICP-OES and IC analysis of electrolyte after immersion at 80°C.

Element/Ion	Unit	Fresh reference	Stored reference	EPDM 1	EPDM 2	FKM 1	FKM 2
Al, B, Ba, Br^-, Cl^-, Co, Cr, Cu, Fe, K, Mg, Mn, Mo, Na, Ni, Pb, SO_4^{3-}, Ti, Zn	mg/kg	-	-	-	-	-	-
Ca	mg/kg	-	-	-	-	-	5
Si	mg/kg	-	-	4	-	-	6
DFP^-	wt. %	0.01	0.1	0.34	0.07	0.17	0.41
PF_6^-	wt. %	12.4	12.4	12.7	12.4	12.3	11.4

In the HPLC-MS measurement, the stored reference showed clearly detectable additional peaks compared to the fresh reference (

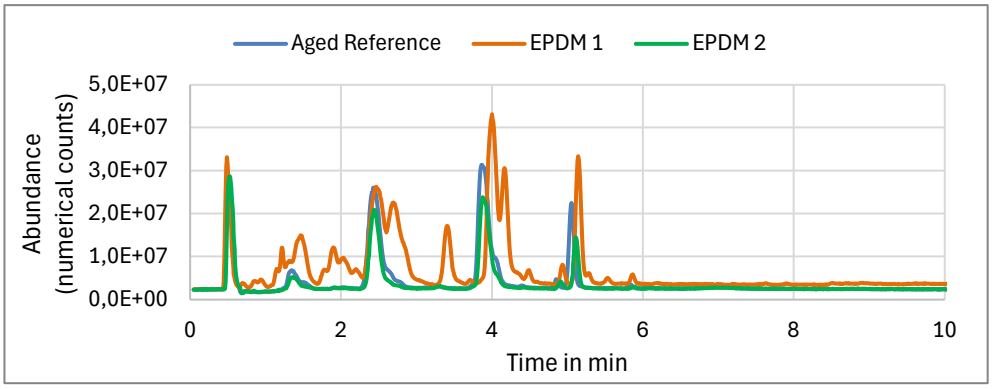

Figure 9). These consist of carbonate oligomers and could be due to VC polymerization. The chromatographs for FKM 1 and EPDM 2 look identical to the stored reference, so no other organic leach-out or reaction products existed.

FKM 2 and EPDM 1, on the other hand, showed additional peaks that match different phosphate signals, again confirming the underlying reaction.

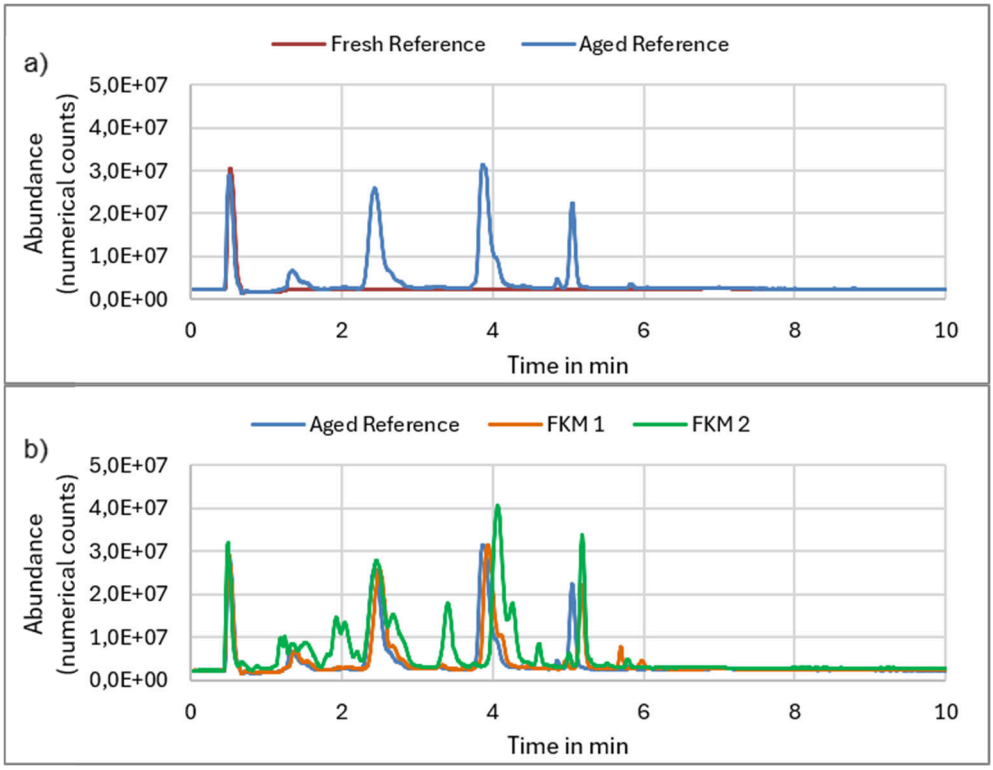

c)

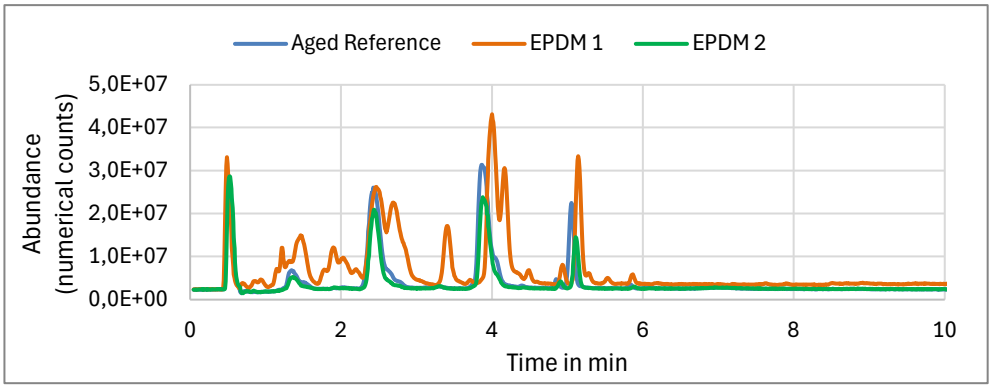

Figure 9: HPLC-MS chromatogram of the a) Fresh and aged reference, b) Electrolyte after storage of FKM 1 and FKM 2, c) Electrolyte after storage of EPDM 1 and EPDM 2.

5.3 Effect on Battery Performance

The relative discharge capacity, shown in Figure 10, was normalized to the eighth cycle, corresponding to the first cycle at 1C, and must be interpreted in conjunction with the absolute discharge capacity. Here, 1C denotes a current rate at which the cell is fully charged or discharged within 1 hour.

Considering cell-to-cell variation, all electrolytes exhibited similar and stable absolute discharge capacity retention, reaching approximately 240 mAh after 300 cycles. Cells containing the fresh reference electrolyte showed a slightly higher absolute capacity during the first 50 cycles compared to those with aged electrolytes, while cells with EPDM 1 and FKM 2 displayed the lowest absolute capacities within the first 20 cycles.

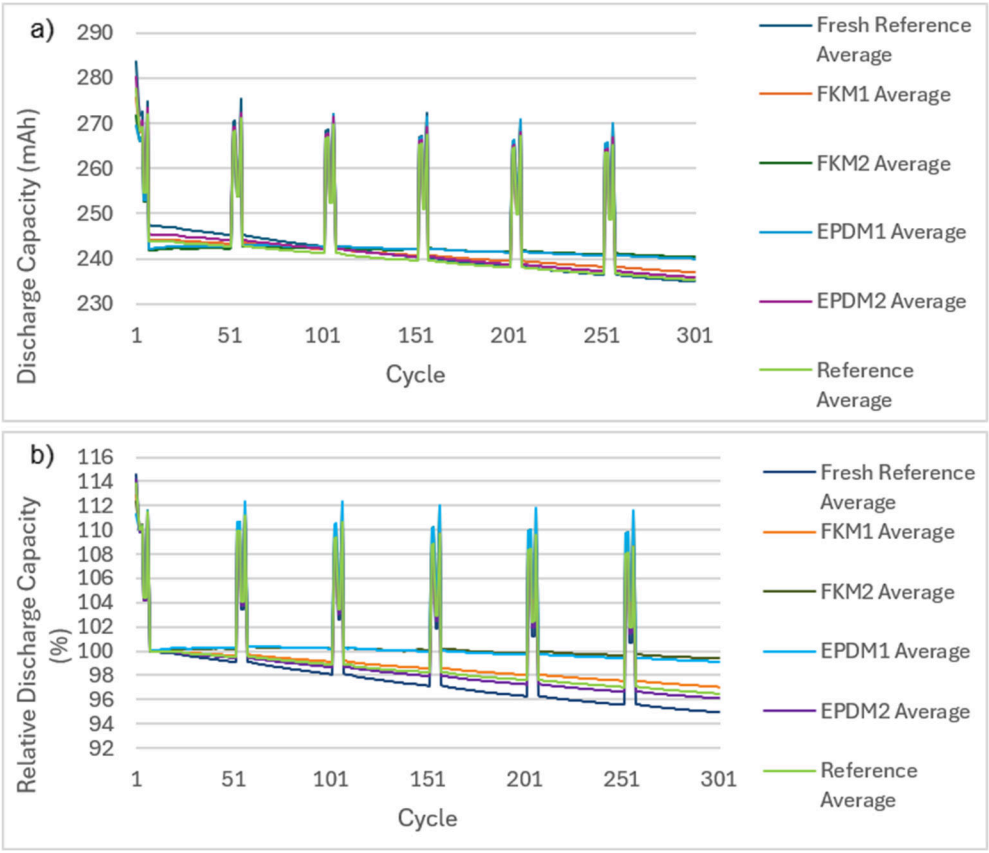

Figure 10: Discharge capacity (a) and relative discharge capacity (b) of fresh and aged electrolytes during the cycling process.

After 300 cycles, all electrolytes achieved a relative discharge capacity between 95 % and 99 %. The cells with EPDM 1 and FKM 2 demonstrated the highest relative

capacity retention, with almost no fading observed during the first 150 cycles. Overall, the electrolytes showed a gradual increase in capacity loss in the following order: FKM 1, reference, EPDM 2 and fresh reference.

Relative discharge capacity is directly related to the DFP^- content measured in the IC and shown in Table 4, which is the result of the decomposition process. In this case, the higher the content, the better the cell performance, or in other words, the higher the remaining relative discharge capacity. In some electrolyte recipes, DFP is added as an additive to improve capacity and cyclability. As it was not added in the base recipe, here it is still a sign of an unwanted degradation process.

All cells exhibited an increase in internal resistance, shown in Figure 11, over the course of cycling. The cells containing the fresh reference electrolyte and FKM 1 showed similar behavior and the lowest internal resistance values.

In contrast, cells with FKM 2, EPDM 1, EPDM 2 and the reference electrolyte displayed higher internal resistance values. These groups also showed greater variability, except for EPDM 1, which exhibited comparatively consistent results.

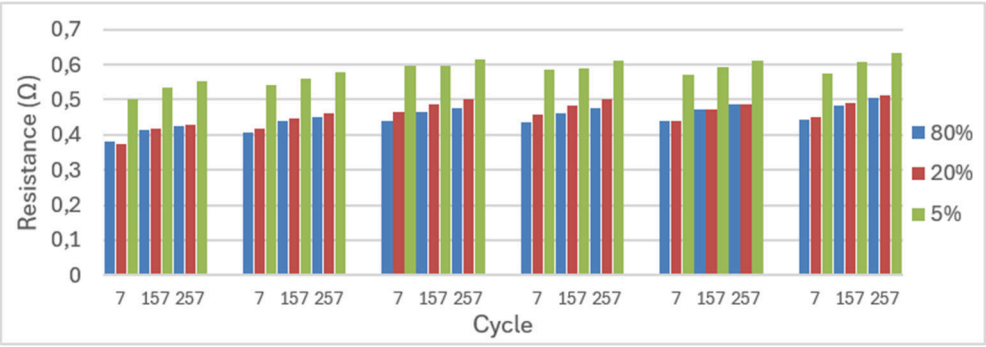

Figure 11: Average internal resistance of fresh and aged electrolytes during cycling process.

6 Summary and Conclusion

This study demonstrates that elastomer-electrolyte interactions in $LiPF_6$-based lithium-ion battery systems depend heavily on both polymer type and filler chemistry, and can significantly influence electrolyte stability and, indirectly, battery performance.

Clear differences were observed between EPDM and FKM material. EPDM systems exhibited low swelling but showed strong dependence on filler type.

The silica-filled EPDM 1 showed severe degradation at +80 °C, including surface crust formation, significant mechanical property loss and strong interaction with the electrolyte. In contrast, the carbon-black-filled EPDM 2 showed minimal reactivity, stable mechanical properties and the least impact on electrolyte composition and color.

FKM systems showed strong swelling, indicating high electrolyte uptake and significant transport of reactive species into the polymer network. The silica-filled FKM 2 exhibited internal reactions throughout the material, leading to filler consumption, the formation of phosphorus-rich clusters and mechanical degradation. The barium-based FKM 1 showed mostly reversible swelling effects, limited chemical reaction and comparatively stable filler structure.

Electrolyte analysis revealed that elevated temperature drives significant electrolyte decomposition, even without elastomer contact, as seen in the stored reference. The observed behavior is consistent with a self-accelerating decomposition mechanism.

Electrochemical testing showed that despite strong chemical differences, all cells retained 95–99% capacity after 300 cycles, indicating that short-term performance is only moderately affected. However, differences in internal resistance and early-cycle behavior clearly reflect the underlying electrolyte degradation and impurity formation.

Future work will focus on material optimization and accelerated aging under elevated temperatures and high-SOC storage to promote degradation and identify early failure mechanisms. Complementary post-mortem and corrosion studies will further elucidate processes such as HF-induced aluminum current collector dissolution.

7 Nomenclature

Variable	*Description*	*Unit*
Q	Capacity	[Ah]
R_i	Internal Resistance	[Ω]
T	Temperature	[°C]

8 References

[1] A. Khan, H. Al Rashid, P. K. Roy, S. I. Chowdhury und S. A. Sathi, „Challenges and the Way to Improve Lithium-Ion Battery Technology for Next-Generation Energy Storage," *Energy & Environmental Materials,* 2025.

[2] H. Ritchie, „Tracking global data on electric vehicles," Our World in Data, 20 05 2026. [Online]. Available: https://ourworldindata.org/electric-car-sales. [Accessed May 25, 2026].

[3] „Global EV Outlook 2025: Electric vehicle batteries," Agency, International Energy, [Online]. Available: https://www.iea.org/reports/global-ev-outlook-2025/electric-vehicle-batteries. [Accessed May 25, 2026].

[4] „Electric Vehicle Battery Market (2025 - 2030)," Grand View Research, [Online]. Available: https://www.grandviewresearch.com/industry-analysis/electric-vehicle-battery-market. [Accessed May 25, 2026].

[5] T. Rahman und T. Alharbi, „Exploring Lithium-Ion Battery Degradation: A Concise Review of Critical Factors, Impacts, Data-Driven Degradation Estimation Techniques, and Sustainable Directions for Energy Storage Systems," *Batteries,* Bd. 10, Nr. 220, p. 7, 2024.

[6] S. Lux, S. Lucas, E. Pollak, S. Passerini, M. Winter und R. Kostecki, „The mechanism of HF formation in LiPF6-based organic carbonate electrolytes," *The mechanism of HF formation in LiPF6-based organic carbonate electrolytes,* 2011.

[7] „Enhancing Battery Performance: Utilizing FPI ICP-OES to Accurately Assess Metal Impurities in Electrolytes," Focused Photonics Inc. (FPI), 29 01 2024. [Online]. Available: https://www.environmental-expert.com/news/enhancing-battery-performance-utilizing-fpi-icp-oes-to-accurately-assess-metal-impurities-in-electro-1137046. [Accessed May 28, 2026].

9 Authors

Trelleborg Sealing Solutions
Schockenriedstr. 1, 70565 Stuttgart, Germany

Sandra Kofink, M. Sc., Sandra.Kofink@trelleborg.com

Marc Gay, M. Eng., Marc.Gay@trelleborg.com

https://doi.org/10.61319/LFII7XX4